



Tecnologías, Gestión  
y Biogeoquímica Ambiental  
Universidad de Las Palmas de Gran Canaria



# Identification of marine microplastics collected in the Canary Islands: coastal and oceanic samples

**Sara Isabel Ortiz Montosa**

**Curso 2018/2019**

**Tutora: Daura Vega Moreno**

**Cotutor: Eugenio Fraile Nuez**

Trabajo Fin de Título para la obtención  
del título Grado en Ciencias del Mar

## Identification of marine microplastics collected in the Canary Islands: coastal and oceanic samples

Author: Sara Isabel Ortiz Montosa

Degree: Degree in Marine Science. ULPGC

Tutor: Daura Vega Moreno

Chemistry Department, ULPGC.

Research group: Technologies, Management and Environmental Biogeochemistry  
(TGBA).

Cotutor: Eugenio Fraile Nuez

Instituto Español de Oceanografía (IEO). Santa Cruz de Tenerife.

Student signature:

Tutor signature:

Cotutor signature:

## **INDEX**

<b>ABSTRACT</b>	<b>4</b>
<b>1. INTRODUCTION</b>	<b>5</b>
<b>2. MATERIAL AND METHODS</b>	<b>7</b>
<b>3. EXPERIMENTAL</b>	<b>8</b>
3.1 OPEN WATER SAMPLES	8
3.1.1 STUDY AREA	8
3.2 COASTAL SAMPLE	11
3.2.1 YELLOWNESS INDEX	11
<b>4. RESULTS</b>	<b>13</b>
4.1 OPEN WATER SAMPLES	13
4.2 COASTAL SAMPLES	19
<b>5. DISCUSSION</b>	<b>20</b>
<b>6. CONCLUSIONS</b>	<b>21</b>
<b>7. BIBLIOGRAPHY</b>	<b>22</b>
<b>ANNEX I</b>	<b>25</b>

## **Abstract**

The existence of microplastic in the water column between 50 and 300 meters depth in the Atlantic Ocean is reported for first time. To carry on this study, some cruises near Canary Islands were done. Microplastic concentrations could be related with the density profiles. The samples are taken at different depths in a range of between 0 to 300 meters deep. A rosette with a CTD and 23 Niskin bottles were used to take these samples. Between 100 and 280 meters deep, the highest concentrations of microplastics were found.

On the other hand, we have used samples of coastal microplastic, to study the colour variation of the material due to degradation process. With PANTONE® Studio app it was determined and compared with the plastic composition (determined using FTIR) and its colorimetry (through a colorimeter). With all this data we have calculated the yellowness index value of each sample and compared with Pantone code colour. The values of yellowness index are in a range between the values 17,722 and 127,874%. The optimization of this methodology lets the determination of yellowness index in a simpler way using just a mobile app.

## 1. Introduction

Plastic debris in the marine environment is widely documented. Reports of plastics in the marine environment began to appear in the early 1970s [1,2]. The quantity of plastic entering the ocean from waste generated on land is unknown but has noticeably increased over the recent years [3,4]. Estimates on the amount of plastics are 275 million tons (MT) according to Eriksen et al. (2014) and 245 million tons (MT) according to Andrady et al. (2011) of plastic waste that was generated in 192 coastal countries. For 2015, the prediction models calculated an increase in the order of magnitude of plastic waste in the ocean. This accumulation is due to the lack of proper management planning and infrastructure [3].

For the first time in the 1970s, the presence of small plastic fragments in the open ocean was highlighted [6]. As a result of synergistic effects, the fragmentation of plastic debris can be divided into four main categories: macroplastics ( $\geq 1$  cm), mesoplastics ( $\geq 5$  mm to 1 cm), microplastics ( $\leq 5$  mm) and nanoplastics ( $\leq 100$  nm) [4–6].

Microplastics (MP) constitute a very heterogeneous assemblage of particles that differ in density, shape, chemical composition, size, colour and others. MP can be subdivided by source and usage as “primary” microplastics and “secondary” microplastics. Primary microplastics are produced either for indirect use, as precursors (nurdles or virgin resin pellets) to produce polymer consumer products, or for direct use, such as in cosmetics, scrubs and abrasives. Secondary microplastics derive from the breakdown of larger plastic material into smaller fragments. This fragmentation arises by a combination of mechanical forces like waves and/or photochemical processes generated by sunlight. Some “degradable” plastics are designed to break up into small particles, but the resulting material does not necessarily biodegrade [7].

The composition of some plastic classes is: Polyethylene (PE), Polypropylene (PP), Polystyrene (PS), Poly (ethylene terephthalate) (PET); and Poly (vinyl chloride) (PVC). Polymers with lower density than seawater (e.g. PE and PP) tend to float at the surface, while those that are denser (like PVC) tend to sink, varying their position in the water column due to water fronts or biofouling. Biofouling tends to increase the weight of particles, affecting their buoyancy and accelerating their sinking velocity to the seafloor [4,8]. There is a relationship between wind speed and MPs concentration. One of the causes of the high concentration of MPs could be due to moderate wind conditions, as they sink into the mixed layer and cannot be carried out by surface currents, and the MPs concentration descend with the wind velocity increase, as they now can be carried out by surface currents [9].

The MPs composition, degradation, fragmentation and the leaching of additives, can modify their density and location along the water column, in addition to undergo adsorption of pollutants as POPs [5,6]. These contaminants are widespread and ubiquitous within the marine environment, with the potential to cause damage to biota [10,11]. The little size of the MPs makes them bioavailable to organisms throughout the food-web (Figure 1). Plastic pollution is globally distributed over all oceans, because of their buoyancy and durability. Some toxicants found in the plastic composition are introduced in the environment [12,13], leading some researchers to claim that the synthetic polymers in the ocean should be regarded as hazardous waste [3].

The apparent density of the microplastics can change from the amount of fouling they accumulate, since with the passage of time it has a ballast effect and therefore increases the apparent density [14], and therefore they sink along the water column [15,16] and may even end up in deep water or in sediment [17,18].

Before they finish in the sediment, the plastics undergo a temporary phase of fouling although these plastics had a positive buoyancy and were in surface waters. The plastics are sunk by the grazing, but they can float again [15] until they finish in deep waters or sediments [19].

Therefore, the ingestion of microplastics may be introducing toxins to the base of the food chain, from where there is a potential for bioaccumulation [13]. Marine organisms may confuse MPs food or indirectly ingest MPs through preys that were previously contaminated. Microplastics ingestion by marine biota implicate a variety of consequences, such as a reduction of stomach storage capacity, harmed satiation feeling, and distorting feeding behaviour. Moreover, microplastics ingestion can also cause internal lesions in gastrointestinal tracts (e.g. perforated gut or gastric rupture), mainly until death [20].

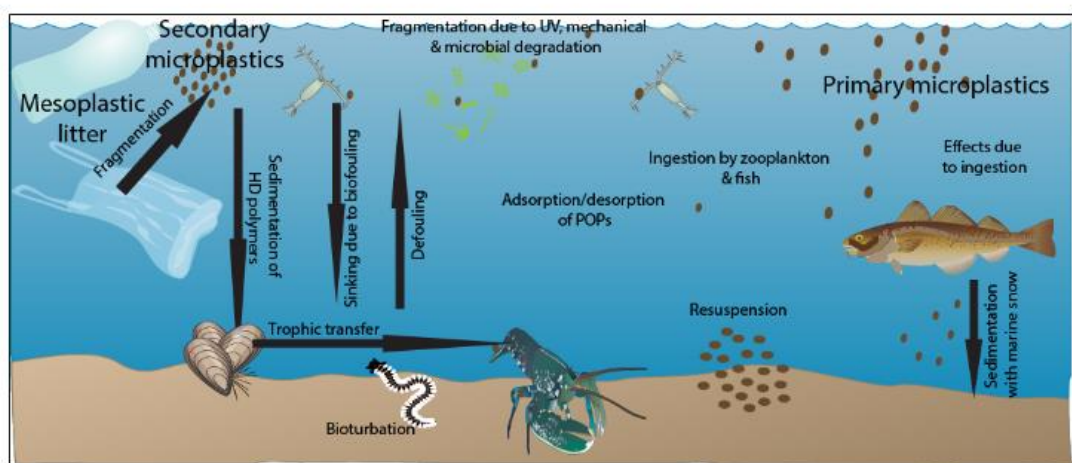


Figure 1. Interaction of the microplastic in the food-web [21]

Our study area was around Canary Islands, specifically the Canary Current region, which is located off the northwestern coast of Africa in the Atlantic Ocean. The southward flow and the seasonal variability of the Canary Current bring plastic debris from the open North Atlantic Ocean to the coasts of the Canary Islands, mainly on the N and NE exposed beaches [22]. In addition, the islands are located in the subtropical turn of the North Atlantic [23]. According to Brach et al., (2018) it associates the eddies of the North Atlantic Gyre with the microplastics presence. So, it shows that both the anticyclonic eddies and the cyclonic eddies can capture material drifting at the surface by introducing them and not letting them escape in the water column.

Most of the previously published studies in this area, confirmed the presence of microplastics in coastal waters [22,24] or in marine organisms [25]. The scientific community focused on superficial (buoyance) and deep (non-buoyance) microplastics. Publish at June 2019, in Nature magazine [26], it was report by first time the accumulation of microplastics in the water column for the Pacific ocean, with higher concentration between 200 and 600 meters depth. In order to determinate the distribution of microplastics in the water column, Samples collected during the PLOCAN 19-1 and VULCANA 0319 cruises, is what my study includes, but to reinforce this study we have used the samples collected in cruises carried out since 2017 [27].

The objectives of this work were two: Determine the presence of microplastic in the water column in samples collected in the open sea.

Determine the yellowness index from microplastics collected on the coast, considering the composition, colorimetry and PANTONE®.

## **2. Material and methods**

The samples are collected with a rosette composed of a CTD (conductivity, temperature and density) that collects the profile of both the rosette descent and rise, and 24 niskin bottles which are used for the collection of water samples. Each niskin bottle has a capacity of 12 litres.

For the collection of samples, a mesh with a size of 100µm as used. A 30x30 cm collector has been manufactured by joining the mesh where the silicone tubes are connected to the niskin bottle outlet and to the collector and concentrated on Whatmann GF / F 47 mm glass fiber filters. Milli Q water (Millipore®) was used to clean the mesh.

The filter contents were classified and quantified under a binocular microscope VWR®.

A needle was used for collecting the most significant fibers and microplastic and wrapped in an aluminium foil individually. Once wrapped it was introduced into a vial and labelled.

The colour classification according to PANTONE® Studio Pantone B2B Licensing incorporates the Pantone colour system in different products and services. PANTONE® Studio consists of a mobile application

To obtain the composition of the plastics we use the FTIR, which is an Agilent technologies® FTIR 630 spectrophotometer. To determine the colorimetry, a VSC500 videocompactor from Foster + Freeman was used.

### **3. Experimental**

#### **3.1 Open water samples**

The samples used in this work are those collected by me during this year, February and March 2019. In addition, samples collected previously, since 2017 [22] , have been processed. This present study demonstrate the existence of microplastics on the water column in open water [28].

##### **3.1.1 Study area**

A total of 5 cruises were carried out for the collection of microplastic which were collected by Rosette between 5 a 300 meters depth around Canary Island, Central-East Atlantic (Figure 2).



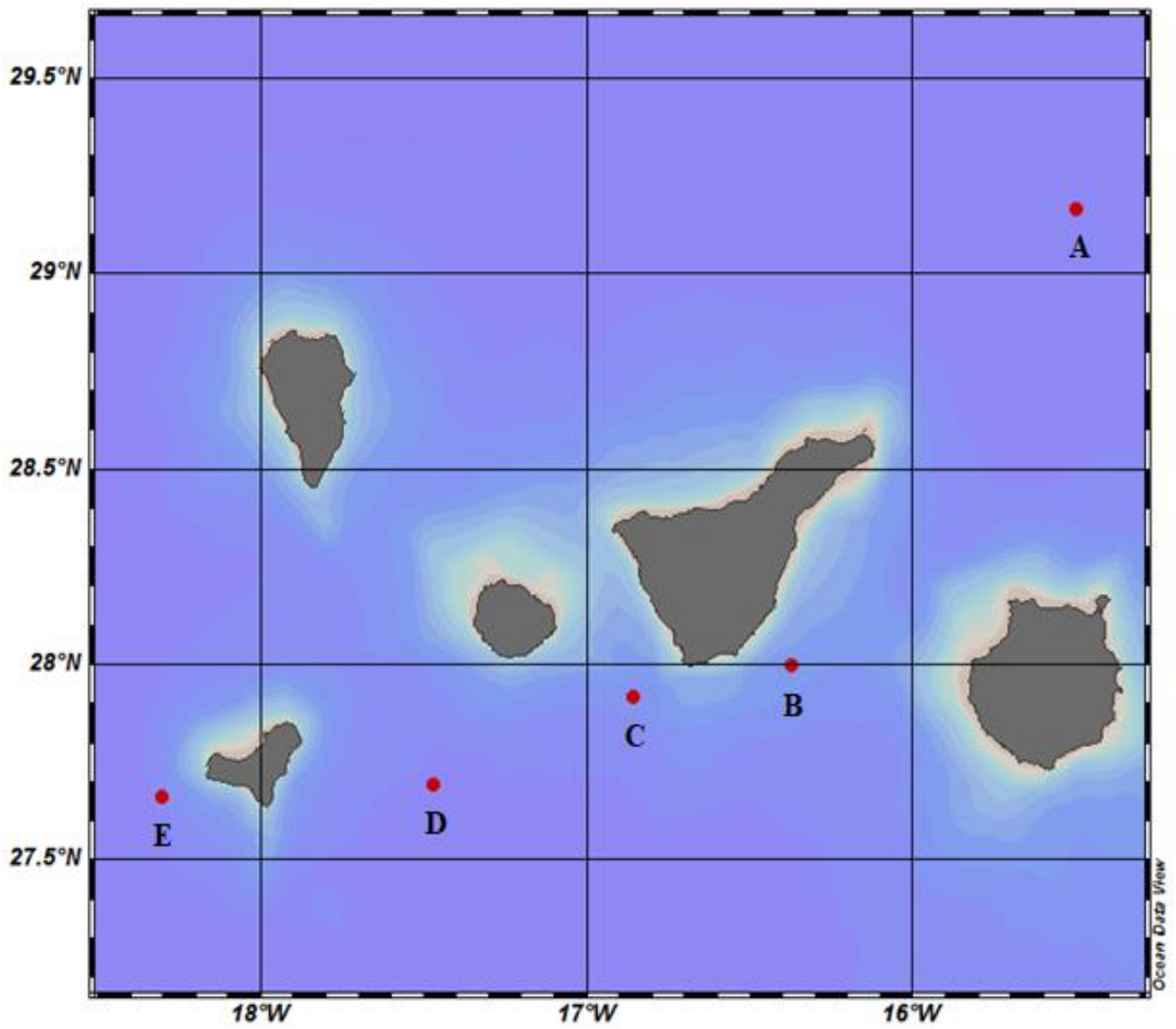


Figure 2. Sampling stations map. A) ESTOC; B) Volcán del Medio; C) Tenerife - Gomera; D) Tenerife – El Hierro; E) Mar de las Calmas ([29]).

The samples were taken in surface, layer of mixture and to maximum 300 meters depth (Table 1).

*Table 1. Cruises carried out from April 2017 to March 2019, sampling stations and depths samples collected.*

Cruise	Station	Station code	Date (month / year)	Depth (m)
PLOCAN 17-1	ESTOC	A	April / 2017	5 ; 50 ; 100 ; 150
PLOCAN 17-2	ESTOC		November / 2017	5 ; 50 ; 100 ; 150
PLOCAN 18-2	ESTOC		December / 2018	5 ; 80 ; 200 ; 350
PLOCAN 19-1	ESTOC		February / 2019	5 ; 108 ; 195 ; 258
VULCANA 0319	Volcán del Medio	B	March / 2019	5 ; 105 ; 178 ; 245
	Tenerife – Gomera	C	March / 2019	5 ; 175 ; 237 ; 292
	Tenerife – El Hierro	D	March / 2019	5 ; 98 ; 130 ; 222 ; 0-300
	Mar de las Calmas	E	March / 2019	5 ; 168 ; 245 ; 280 ; 0-300

In this study, instead of using 24 Niskin bottles, we used 23 bottles of 12 litres each for the extraction samples. The rosette reaches a maximum of 300 meters deep. Once the descent begins, and therefore, the profile is made, the closing depths of each bottle will be decided according to density profile. Four points were chosen in the density profile to close the Niskin bottles. These points are chosen for the change in the density gradient (Figure 5). We closed 6 bottles per chosen depth, except at the depth of 5 meters we closed 5 bottles. This makes a total of 72 litres filtered per sample.

In the VULCANA 2019 cruise, in stations D and E, a mesh is placed inside a niskin bottle, which will not close at any depth, which allows to collect all the possible microplastic of the water column (0-300m). This makes a total of 712.75 litres filtered by station.

The samples of water collected at the same depth were filtered and frozen (-80°C). A total of 4 or 5 filters per station was obtained, which corresponds to 1 filter per sample. The filter samples were transported to the laboratory and defrosted.

The collection of microplastics from the water column is based on a filtration by gravity through a mesh with a pore size of 100 µm. A collector of 30x30cm has been

made by joining the mesh where silicon tubes are connected to the outlet of the niskin bottle and to the collector. All water collected in the Niskin bottle is passed through this mesh, separating it by depths. This mesh is collected in a funnel and cleaned with Milli Q water by passing it through a filter train with a Whatmann GF / F glass fiber filter of 47mm. The content of the sample is retained in the filter, which is placed in a glass Petri dish, labelled and stored at -80°C until analysis.

The procedure for the rest of the cruises is the same as that used for the ESTOC-21 cruises.

## 3.2 Coastal sample

Different microplastics samples collected at Fuerteventura island were classified according to their colour determined by PANTONE® Studio app. Moreover, they were analysed by infrared (FTIR) and colorimetry spectra by reflectance.

PANTONE® Studio app has been used because it provides a universal colour code. Thus, this will allow anyone to identify the colour of the plastics, and in our case, specifically, microplastic colour.

The use of FTIR allows to detect the composition of plastics [30]. In addition, a manual classification is required before the FTIR analysis [17].

The colorimeter allows to convert and calibrate the spectra that are shown by an object that has colour. To do this, it uses the dispersion of the wavelength provided by a variable wavelength filter [31].

For the analysis with PANTONE® Studio, the mobile application was used, and it were obtaining the PANTONE® Studio code from each sample. For this it was necessary to take a picture of each of the samples and determine both PANTONE® Studio and RGB values (red, green and blue). RGB is the composition of colour in terms of the intensity of the primary colours of light, with which it is possible to represent a colour by mixing by adding the three colours

### 3.2.1 Yellowness index

By cause of the oxidation of the microplastic it changes its colour turning from yellow to orange yellow and even dark orange and brown. Due to the thermal stabilizers, which are used in the resin, as products accumulated by the degradation of the polymer

itself, yellowing occurs. This occurs both during the manufacture of the pellet or to the subsequent composition [19].

Yellowness Index (YI) according to ASTM D 1925-70 or E 313- 15e1 is a mathematical expression that allows to quantify this colour change in plastics.

The colour is quantified using coordinates in a three-dimensional colour space proposed by CIE where the vertical axis (L) corresponds to the clarity of the colour, the position of the colour on a two-dimensional surface is defined by "a" and "b", where the gray corresponds "a" = 0 and "b" = 0 (Figure 3) [19].

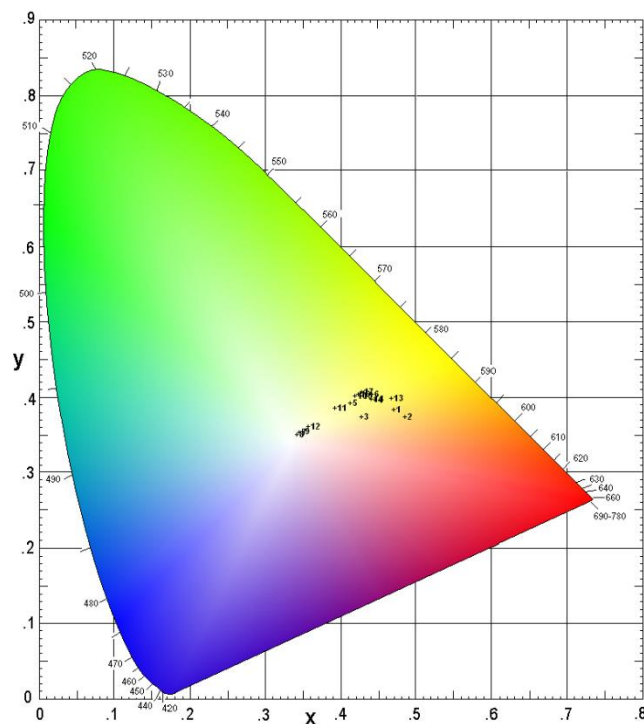


Figure 3. CIE 1931 spectrum obtained from the colorimeter after analysing 20 samples

Yellowness Index (YI E313) is associated with scorching, soiling, and general product degradation by light, chemical exposure, and processing. According to the method ASTM E131, where the result obtained is a percentage (%). It is calculated:

$$YI E313 = 100 \frac{C_X X - C_Z Z}{Y} \quad (I)$$

Where, x, y and z are values of CIE Tristimulus (Figure 3) and the coefficients depend on the luminosity [32]. X, Y, Z are the values that are the perfect reflective diffusion (or clean air) of the combination of observation / luminosity. Where Y is the

luminance [33]. Moreover,  $x$ ,  $y$  are the luminosity factor and the chromatic coordinates of the sample [34]. The constants used were for  $C_x= 1.2769$  and  $C_z=1.0592$  [32].

In 1957 ASTM requested new equations for the calculation of Yellowness and the Hunter equation was converted to CIE tristimulus [35]. The International Commission on Illumination (Commission Internationale d'Eclairage: CIE) defined, in 1931, the Standard Observer for Colorimetry and the System of Colorimetry (CIE, 1931) [36].

For the calculation of YI, it is necessary to know X, Y, Z and although this data was provided by the colorimeter, the equations are the following:

$$X = \frac{Y}{y} x \quad (\text{II})$$

$$Y = \frac{xy}{x} \quad (\text{III})$$

$$Z = \frac{Y}{y} (1 - x - y) \quad (\text{IV})$$

Where,  $x$  and  $y$  are the cut with the exes [37].

## 4. Results

### 4.1 Open water samples

In then take down of the CTD density profiles were obtained. From the density profile, different changes were seen in the profile, which determined the closing depths of Niskin bottles (Table 2, 3, 4 and Figure 6). The content of the filter was classified and counted according to composition (Figure 4) and colours:

(1) Composition into different categories: Fibers: (1.1) Group of fibers, (1.2) Individual Fibers, (1.3) Nylon, (1.4) Microplastics.

(2) Colours into different categories: (2.1) Transparent, (2.2) White, (2.3) Yellow, (2.4) Brown, (2.5) Red, (2.6) Green, (2.7) Blue, (2.8) Gray, (2.9) Black. The classification by colour was determined subjectively.

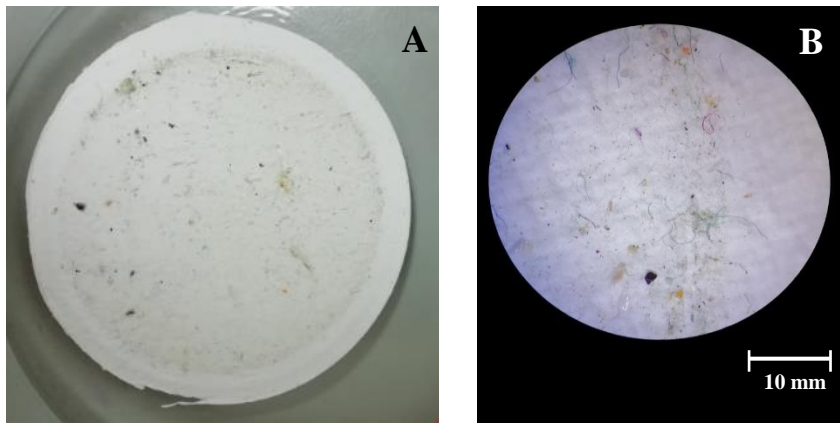


Figure 4. A) Whatmann GF / F 47 mm glass fiber filters. No magnify; B) Picture took under binocular microscope. Both pictures are from station E, sampling belonging to the water column (300 to 0 meters).

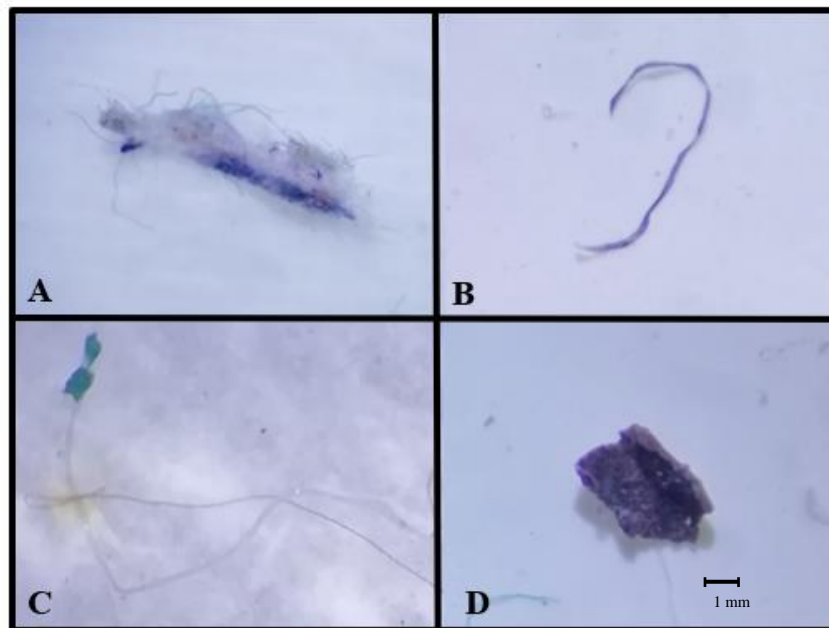


Figure 5. A) Group of fibers. Collected in station B, VULCANA 0319, at 178 meters deep. B) Individual fiber. Collected in station D, VULCANA 0319, at 222 meters deep. C) Nylon. Collected in station A, ESTOC April 2017, at 50 meters deep. D) Microplastic. Collected in station E, VULCANA 0319, at 280 meters deep.

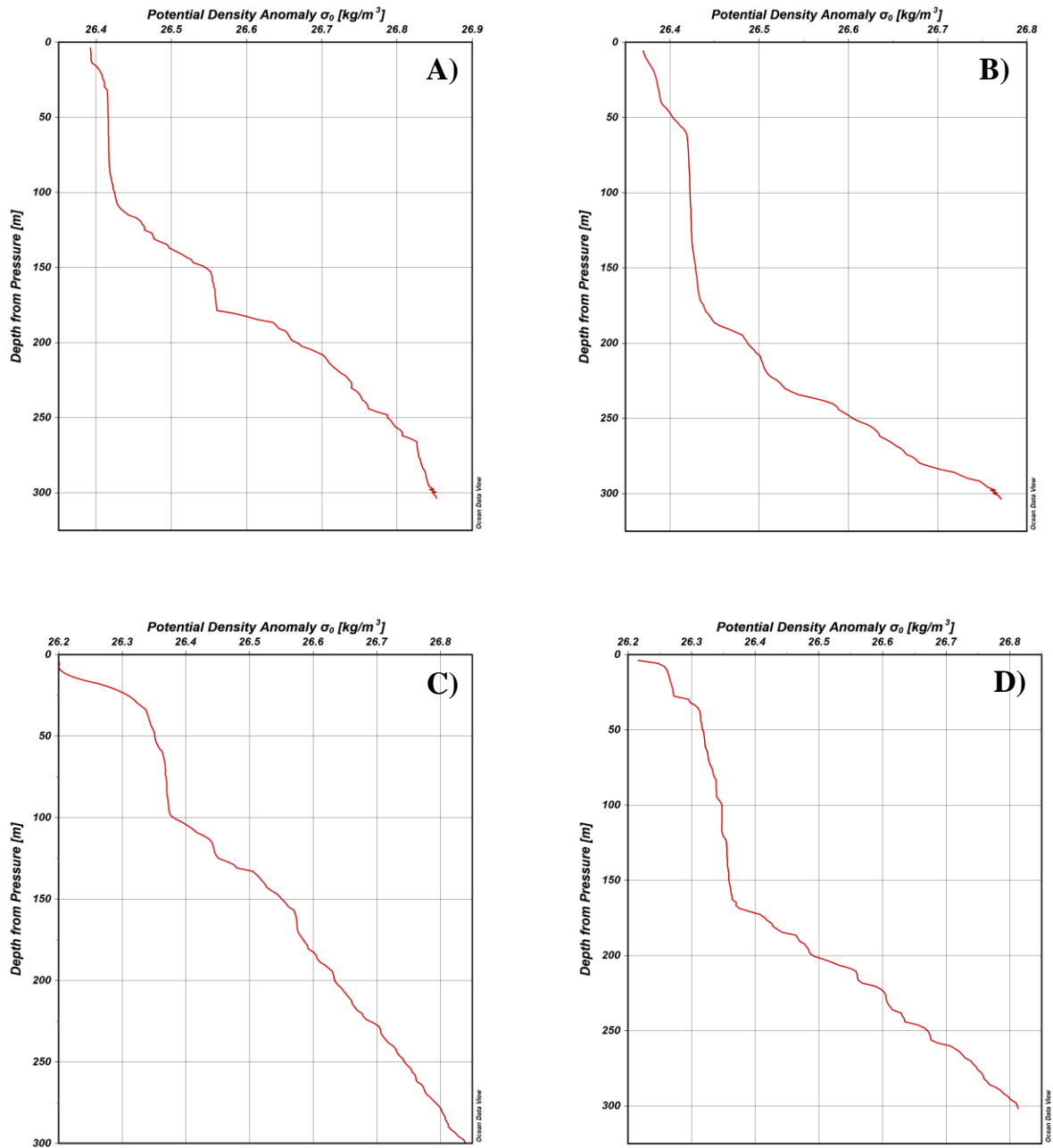


Figure 6. Vertical profiles of seawater density measured in the VULCANA cruise in March 2019. A) Volcán del Medio; B) Tenerife - Gomera; C) Tenerife - El Hierro; D) Mar de las Calmas. [31]

Table 2. Classification of samples according to depth and composition. ESTOC cruises

<b>ESTOC</b>		<b>DEPTH [m]</b>			
<b>April 2017</b>					
<b>Composition</b>	<b>-5</b>	<b>-50</b>	<b>-100</b>	<b>-150</b>	
Group of fibers	2	3	-	2	
Individual fiber	13	27	40	33	
Nylon	-	1	-	-	
Microplastics	2	5	73	9	
<b>ESTOC</b>		<b>DEPTH [m]</b>			
<b>November 2017</b>					
<b>Composition</b>	<b>-5</b>	<b>-50</b>	<b>-100</b>	<b>-150</b>	
Group of fibers	-	1	-	-	
Individual fiber	12	7	13	29	
Nylon	-	-	-	1	
Microplastics	6	1	5	4	
<b>ESTOC</b>		<b>DEPTH [m]</b>			
<b>December 2018</b>					
<b>Composition</b>	<b>-5</b>	<b>-50</b>	<b>-100</b>	<b>-150</b>	
Group of fibers	-	1	-	-	
Individual fiber	38	73	110	60	
Nylon	-	-	-	-	
Microplastics	2	4	4	7	
<b>ESTOC</b>		<b>DEPTH [m]</b>			
<b>February 2019</b>					
<b>Composition</b>	<b>-5</b>	<b>-108</b>	<b>-195</b>	<b>-258</b>	
Group of fibers	-	1	-	1	
Individual fiber	7	14	11	13	
Nylon	-	-	-	-	
Microplastics	3	2	-	13	



Table 3. Classification of samples according to depth and composition. VULCANA cruise.

<b>VULCANA</b>		<b>DEPTH [m]</b>				
<b>Mar de las Calmas</b>						
<b>Composition</b>	<b>-5</b>	<b>-168</b>	<b>-245</b>	<b>-280</b>	<b>0-300</b>	
Group of fibers	1	2	1	3	>10	
Individual fiber	35	16	42	117	>300	
Nylon	-	-	-	-	-	
Microplastics	4	2	3	7	54	

<b>VULCANA</b>		<b>DEPTH [m]</b>				
<b>Tenerife – El Hierro</b>						
<b>Composition</b>	<b>-5</b>	<b>-98</b>	<b>-130</b>	<b>-222</b>	<b>0-300</b>	
Group of fibers	1	5	-	1	3	
Individual fiber	27	41	61	87	231	
Nylon	-	-	-	-	-	
Microplastics	-	2	-	3	101	

<b>VULCANA</b>		<b>DEPTH [m]</b>			
<b>Tenerife – Gomera</b>					
<b>Composition</b>	<b>-5</b>	<b>-175</b>	<b>-237</b>	<b>-292</b>	
Group of fibers	3	3	4	-	
Individual fiber	216	210	121	46	
Nylon	-	-	-	-	
Microplastics	5	8	2	4	

<b>VULCANA</b>		<b>DEPTH [m]</b>			
<b>Volcán del Medio</b>					
<b>Composition</b>	<b>-5</b>	<b>-105</b>	<b>-178</b>	<b>-245</b>	
Group of fibers	3	3	5	1	
Individual fiber	56	104	55	70	
Nylon	-	-	-	-	
Microplastics	10	4	6	5	

*Table 4. Classification of the microplastics in the water column (0-300m) according to the colour.*

<b>VULCANA</b>		
<b>Mar de las Calmas</b>		
<b>Colour</b>	<b>Microplastic</b>	<b>Fibers</b>
Transparent	6	1
White	2	-
Yellow	7	-
Brown	9	-
Red	2	3
Green	13	>150
Blue	5	>150
Gray	10	-
Black	-	11

Specific analyses of the composition of plastics will be carried out, but these analyses are not the subject of this TFG.

## 4.2 Coastal samples

The result obtained when using the colorimeter is a CIE spectrum (Figure 7), which concedes to graphically present the chromaticity of the colours. Additionally, a range of colours has been made to identify a range of PANTONE® Studio with its respective YI (Figure 8).

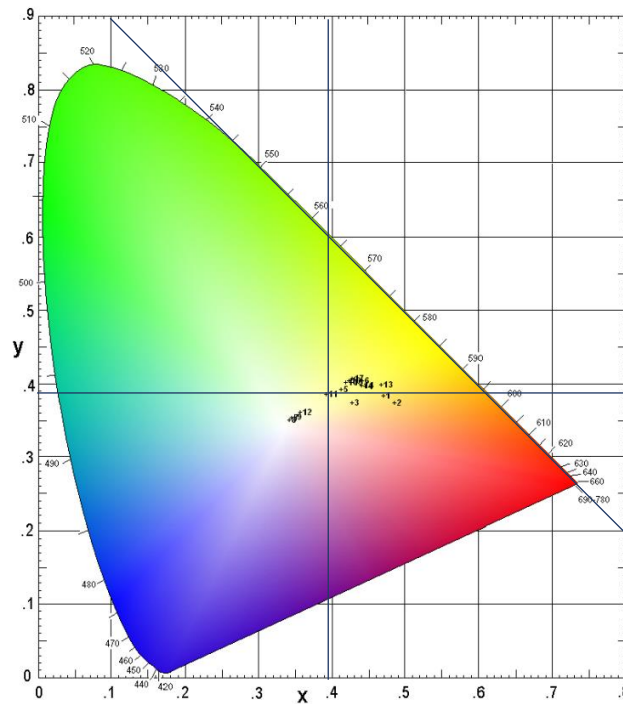


Figure 7. CIE 1931 spectrum. Example of a sample with the cuts  $x$ ,  $y$  and  $z$ , where  $z$  is the tangent.

Both  $x$ ,  $y$  and  $z$  are provided by the colorimeter.  $X$ ,  $Y$  and  $Z$  were calculated using equations (II), (III) and (IV) (section 3.2.1).

With these results and knowing that pantone has the sample analysed, we can determine the YI of each sample and have a colour palette as the figure 8.

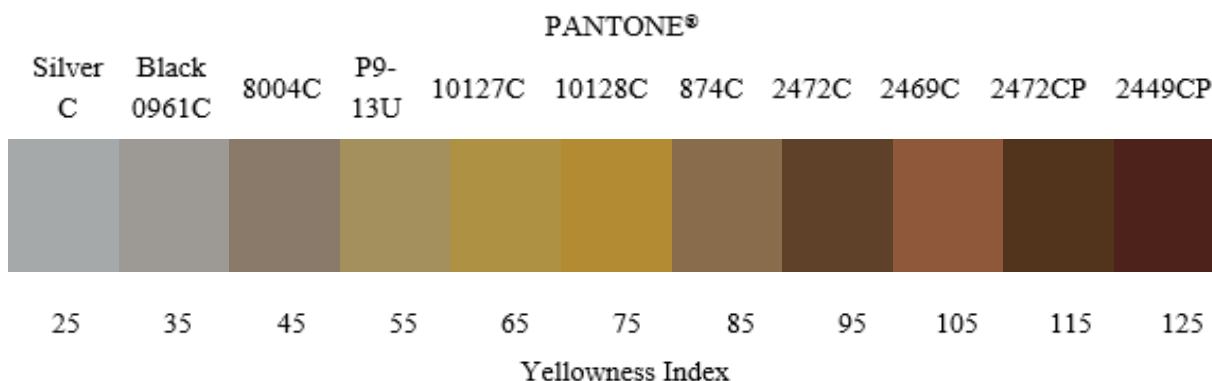


Figure Colour range to determine the yellowness index from the pantone of the microplastic.

Due to the limitations of the offices programs, the colour range is not represented as in the application PANTONE® Studio.

## 5. Discussion

In all the cruises carried out at ESTOC at the depth that we find the greatest amount of both MP and fibers is at 100 meters deep (Table 2 and 3).

In the VULCANA cruise, in all stations, the greatest number of fibers and microplastics are found below 100 meters depth, reaching 280 meters depth in Mar de las Calmas, station E and 105 meters depth in Volcán del Medio, station B.

Regarding colour, the most abundant fibers found are green and blue. More than 150 blue fibers and more than 150 green fibers have been found in the water column (Table 4). However, the most abundant colour in microplastics are green and gray. 13 MP green and 10 MP gray were identified in the water column. The microplastic found in the water column has a lower density than that of seawater, so it should be on the surface.

Another reason the MP is in the column is by cause of the vertical distribution. There is a relationship between the concentration of MP and its mass, which decreases exponentially with depth, considering that the calmer the ocean is and the greater the size of the larger particle is this decrease.

Below is a range of the colours obtained (Figure 7) when analysing the PANTONE® Studio of the samples and associating it with their respective YI. The proposed scale

represents an example, but it will be sent to a designer and it will be done more accurately and with a higher quality, than can be exportable to other researchers in an open repository.

Regarding the relevant calculations to know the YI of the samples and the results obtained range between 17.722 the minimum value and 127.874 the maximum value. The results can be found in ANNEX I.

## **6. Conclusions**

It is the first time in the Atlantic Ocean that it shows that there is microplastic in the water column, besides being very incipient studies that require its expansion.

There is a direct relationship between the differences in the density gradient that marks a density profile with the existence of microplastic at this point.

The determination of YI is a tedious methodology to apply, it requires specific technology such as a colorimeter. The aim of this study is use a simple mobile application which have a huge range of colours with their respective PANTONE® Studio, and then, extrapolate and determine the YI.

## 7. Bibliography

- [1] D.K.A. Barnes, F. Galgani, R.C. Thompson, M. Barlaz, Accumulation and fragmentation of plastic debris in global environments, *Philos. Trans. R. Soc. B Biol. Sci.* 364 (2009) 1985–1998. doi:10.1098/rstb.2008.0205.
- [2] C.W. Fowler, Marine debris and northern fur seals: a case study., *Mar. Pollut. Bull.* 18 (1987) 326–335.
- [3] M. Eriksen, L.C.M. Lebreton, H.S. Carson, M. Thiel, C.J. Moore, J.C. Borerro, F. Galgani, P.G. Ryan, J. Reisser, Plastic Pollution in the World's Oceans: More than 5 Trillion Plastic Pieces Weighing over 250,000 Tons Afloat at Sea, *PLoS One.* 9 (2014) 1–15. doi:10.1371/journal.pone.0111913.
- [4] A.L. Andrady, Microplastics in the marine environment, *Mar. Pollut. Bull.* 62 (2011) 1596–1605. doi:10.1016/j.marpolbul.2011.05.030.
- [5] M. Cole, P. Lindeque, C. Halsband, T.S. Galloway, Microplastics as contaminants in the marine environment: A review, *Mar. Pollut. Bull.* 62 (2011) 2588–2597. doi:10.1016/j.marpolbul.2011.09.025.
- [6] A. Cincinelli, T. Martellini, C. Guerranti, C. Scopetani, D. Chelazzi, T. Giarrizzo, A potpourri of microplastics in the sea surface and water column of the Mediterranean Sea, *TrAC Trends Anal. Chem.* 110 (2018) 321–326. doi:10.1016/j.trac.2018.10.026.
- [7] P.K. Roy, M. Hakkarainen, I.K. Varma, A.C. Albertsson, Degradable polyethylene: Fantasy or reality, *Environ. Sci. Technol.* 45 (2011) 4217–4227. doi:10.1021/es104042f.
- [8] D. Lobelle, M. Cunliffe, Early microbial biofilm formation on marine plastic debris, *Mar. Pollut. Bull.* 62 (2011) 197–200. doi:10.1016/j.marpolbul.2010.10.013.
- [9] T. Kukulka, G. Proskurowski, S. Morét-Ferguson, D.W. Meyer, K.L. Law, The effect of wind mixing on the vertical distribution of buoyant plastic debris, *Geophys. Res. Lett.* 39 (2012) 1–6. doi:10.1029/2012GL051116.
- [10] M.R.W. Rands, W.M. Adams, L. Bennun, S.H.M. Butchart, A. Clements, D. Coomes, A. Entwistle, I. Hodge, V. Kapos, J.P.W. Scharlemann, W.J. Sutherland, B. Vira, Biodiversity Conservation: Challenges Beyond 2010, *Science* (80-. ). 329 (2010) 1298–1303. doi:10.1126/science.1189138.
- [11] R.W. Sutherland, P.R. Dunning, W.M. Baker, Amphibian encounter rates on roads with different amounts of traffic and urbanization, *Conserv. Biol.* 24 (2010) 1626–1635. doi:10.1111/j.1523-1739.2010.01570.x.
- [12] Y. Mato, T. Isobe, Moore-Plastic\_Resin\_1\_, 35 (2001) 318–324.
- [13] E.L. Teuten, S.J. Rowland, T.S. Galloway, R.C. Thompson, Potential for plastics to transport hydrophobic contaminants, *Environ. Sci. Technol.* 41 (2007) 7759–7764. doi:10.1021/es071737s.
- [14] A. Cózar, F. Echevarría, J.I. González-Gordillo, X. Irigoien, B. Ubeda, S. Hernández-León, A.T. Palma, S. Navarro, J. García-de-Lomas, A. Ruiz, M.L.

- Fernández-de-Puelles, C.M. Duarte, Plastic debris in the open ocean., *Proc. Natl. Acad. Sci. U. S. A.* 111 (2014) 10239–44. doi:10.1073/pnas.1314705111.
- [15] Y. Song, A. Landrady, Fouling of floating plastic debris under Biscayne Bay exposure conditions, *Mar. Pollut. Bull.* 22 (1991) 608–613.
- [16] F.M.C. Fazey, P.G. Ryan, Biofouling on buoyant marine plastics: An experimental study into the effect of size on surface longevity, *Environ. Pollut.* 210 (2016) 354–360. doi:10.1016/j.envpol.2016.01.026.
- [17] M. Claessens, S. De Meester, L. Van Landuyt, K. De Clerck, C.R. Janssen, Occurrence and distribution of microplastics in marine sediments along the Belgian coast, *Mar. Pollut. Bull.* 62 (2011) 2199–2204. doi:10.1016/j.marpolbul.2011.06.030.
- [18] L.C. Woodall, A. Sanchez-Vidal, M. Canals, G.L.J. Paterson, R. Coppock, V. Sleight, A. Calafat, A.D. Rogers, B.E. Narayanaswamy, R.C. Thompson, The deep sea is a major sink for microplastic debris, *R. Soc. Open Sci.* 1 (2014). doi:10.1098/rsos.140317.
- [19] A.L. Andrady, The plastic in microplastics: A review, *Mar. Pollut. Bull.* 119 (2017) 12–22. doi:10.1016/j.marpolbul.2017.01.082.
- [20] S.J. McCauley, K.A. Bjorndal, Conservation Implications of Dietary Dilution from Debris Ingestion: Sublethal Effects in Post-Hatchling Loggerhead Sea Turtles Implicaciones para la Conservación, Dilución de Dietas por Ingestión de Basura: Efectos Subletales en Crías de la Tortuga Ma, *Conserv. Biol.* 13 (1999) 925–929. <http://dx.doi.org/10.1046/j.1523-1739.1999.98264.x>.
- [21] I.L. Nerland, C. Halsband, I. Allan, K. V. Thomas, Microplastics in marine environments: Occurrence, distribution and effects, 2014. doi:10.1183/09031936.06.00108105.
- [22] J. Baztan, B. Jorgensen, S. Pahl, R.C. Thompson, J.-P. Vanderlinden, *Micro2016*, 2016.
- [23] L. Brach, P. Deixonne, M.F. Bernard, E. Durand, M.C. Desjean, E. Perez, E. van Sebille, A. ter Halle, Anticyclonic eddies increase accumulation of microplastic in the North Atlantic subtropical gyre, *Mar. Pollut. Bull.* 126 (2018) 191–196. doi:10.1016/j.marpolbul.2017.10.077.
- [24] A. Herrera, M. Asensio, I. Martínez, A. Santana, T. Packard, M. Gómez, Microplastic and tar pollution on three Canary Islands beaches: An annual study, *Mar. Pollut. Bull.* (2017) 0–1. doi:10.1016/j.marpolbul.2017.10.020.
- [25] A. Herrera, A. Štindlová, I. Martínez, J. Rapp, V. Romero-Kutzner, M.D. Samper, T. Montoto, B. Aguiar-González, T. Packard, M. Gómez, Microplastic ingestion by Atlantic chub mackerel (*Scomber colias*) in the Canary Islands coast, *Mar. Pollut. Bull.* 139 (2019) 127–135. doi:10.1016/j.marpolbul.2018.12.022.
- [26] C.A. Choy, B.H. Robison, T.O. Gagne, B. Erwin, E. Firl, R.U. Halden, J.A. Hamilton, K. Katija, S.E. Lisin, C. Rolsky, K. S. Van Houtan, The vertical distribution and biological transport of marine microplastics across the epipelagic and mesopelagic water column, *Sci. Rep.* 9 (2019) 7843. doi:10.1038/s41598-019-44117-2.

- 
- [27] D. Vega, Fate and impact of microplastics: knowledge, actions and solutions, in: 2017: p. 421.
- [28] B. Abaroa, J.J. Hernández, L.M. San Emeterio, J.A. González, D. Vega, Determinación de microplásticos y sus contaminantes químicos asociados en función del tipo de plástico: Estudio en costa y en la columna de agua, *Not Publ. Yet.* (n.d.).
- [29] R. Schlitzer, *Ocean Data View user's Guide*, (2016). <http://odv.awi.de>.
- [30] M.G.J. Löder, M. Kuczera, S. Mintening, C. Lorenz, G. Gerdt, Focal plane array detector-based micro-Fourier-transform infrared imaging for the analysis of microplastics in environmental samples, *Environ. Chem.* 12 (2015) 563–581.
- [31] G. Wyszocki, W.S. Stiles, C. Science, L.R. Masten, U. Optronics, T. Instru, United States Patent (19), 1993.
- [32] A. Hunterlab, S.O. Function, Y. Index, A. Method, C.I.E. Tristimulus, Y. Index, Y. Index, A. Method, U. Xe, Yellowness Indices, 8 (2008) 5–6.
- [33] S. Using, H. Geometry, S. Using, B. Geometry, Standard Test Method for Color Determination of Plastic Pellets 1, (n.d.) 1–5.
- [34] C. Evaluation, S. Using, H. Geometry, M.C. Using, Standard Practice for Calculating Yellowness and Whiteness Indices from Instrumentally Measured Color Coordinates 1, (2019) 1–6. doi:10.1520/E0313-15E01.2.
- [35] O. Evaluation, S. Using, H. Geometry, S. Using, B. Geometry, M.C. Using, Standard Practice for Calculating Yellowness and Whiteness Indices from Instrumentally Measured Color Coordinates 1, (n.d.) 4–9.
- [36] J. Shanda, *COLORIMETRY. Understanding the CIE System*, in: Wiley-Interscience, 2007: pp. 1–10.
- [37] D.A. Kerr, The CIE XYZ and xyY Color Spaces, Issue. (2010) 1–16. [http://www.haralick.org/DV/CIE\\_XYZ.pdf](http://www.haralick.org/DV/CIE_XYZ.pdf)  
[http://graphics.stanford.edu/courses/cs148-10-summer/docs/2010--kerr--cie\\_xyz.pdf](http://graphics.stanford.edu/courses/cs148-10-summer/docs/2010--kerr--cie_xyz.pdf).



## ANNEX I

Table 5. Correlation between PANTONE® Studio, composition (FTIR) and colorimeter. Results obtained after applying the formula of YI using the coefficients  $C_x=1.2769$  and  $C_z=1.0592$

<b>PANTONE® Studio</b>	<b>Composition</b>	<b>X</b>	<b>Y</b>	<b>Z</b>	<b>YI</b>
2449CP	Polyethylene, chlorinated	1.007	1.007	1	0
2449CP	Polyethylene, chlorinated	0.245	0.197	0.076	117.940
2449CP	Polyethylene	0.272	0.207	0.078	127.874
2469C	Polyethylene, chlorinated	0.275	0.238	0.125	91.911
2469C	Polyethylene, chlorinated	0.329	0.288	0.114	103.941
2469C	Polyethylene, chlorinated	0.458	0.431	0.215	82.852
10124C	Polyethylene	0.405	0.366	0.141	100.491
10124C	Polyethylene, chlorinated	0.631	0.638	0.547	35.477
10124C	Polyethylene, chlorinated	0.635	0.643	0.567	32.701
2470CP	Polyethylene, chlorinated	0.612	0.612	0.515	38.558
2470CP	Polyethylene, chlorinated	0.483	0.455	0.204	88.058
2470CP	Polyethylene, chlorinated	0.549	0.533	0.310	69.919
3523CP	Polyethylene, high density	0.591	0.589	0.462	45.042
3523CP	Polyethylene, chlorinated	0.304	0.257	0.087	115.186
2472C	Polyethylene, chlorinated	0.385	0.343	0.141	99.784
2472C	Polyethylene, chlorinated	0.429	0.399	0.173	91.366
2472C	Polyethylene, chlorinated	0.416	0.392	0.167	90.384

P6-8U	Polyethylene, chlorinated	0.373	0.351	0.143	92.541
2443U	Polyethylene, chlorinated	0.605	0.609	0.503	39.367
P6-14U	Polyethylene, chlorinated	0.412	0.356	0.131	108.800
P6-14U	Polyethylene, chlorinated	0.584	0.587	0.411	52.875
8024C	Polyethylene, chlorinated	0.588	0.592	0.436	48.819
8044C	Polyethylene, chlorinated	0.369	0.316	0.132	104.861
P8-16U	Polyethylene, chlorinated	0.377	0.329	0.160	94.808
P8-16U	Polyethylene, chlorinated	0.534	0.518	0.295	71.313
10127C	Polyethylene, chlorinated	0.601	0.596	0.350	66.560
10127C	Polyethylene, chlorinated	0.579	0.577	0.369	60.395
P9-15C	Polyethylene, chlorinated	0.542	0.532	0.309	68.569
2443C	Polyethylene, chlorinated	0.582	0.575	0.332	68.087
2443C	Polyethylene, chlorinated	0.410	0.385	0.208	78.757
2472CP	Polyethylene, chlorinated	0.366	0.304	0.076	127.252
2472CP	Polyethylene, chlorinated	0.416	0.374	0.168	94.450
2468CP	Polyethylene, chlorinated	0.277	0.232	0.086	113.194
2468CP	Polyethylene, chlorinated	0.402	0.360	0.133	103.456
874C	Polyethylene, chlorinated	0.504	0.478	0.239	81.675
874C	Polyethylene, chlorinated	0.423	0.397	0.205	81.358
8004C	Polyethylene, chlorinated	0.521	0.508	0.380	51.726

8004C	Polyethylene, chlorinated	0.576	0.567	0.480	40.049
SILVER C	Polyethylene, chlorinated	0.593	0.589	0.508	37.203
2474C	Polyethylene, chlorinated	0.711	0.712	0.738	17.723
2474C	Polyethylene, chlorinated	0.650	0.657	0.633	24.279
871C	Polyethylene, chlorinated	0.616	0.614	0.562	31.156
871C	Polyethylene, high density	0.582	0.583	0.435	48.440
2474U	Polyethylene, chlorinated	0.604	0.596	0.373	63.115
2470UP	Polyethylene, chlorinated	0.691	0.698	0.653	27.318
2470UP	Polyethylene, chlorinated	0.677	0.681	0.564	39.218
P9-14C	Polyethylene, chlorinated	0.632	0.641	0.514	40.963
10128C	Polyethylene, chlorinated	0.513	0.504	0.265	74.278
10128C	Polyethylene	0.511	0.500	0.281	70.972
BLACK 0961C	Polyethylene, chlorinated	0.541	0.529	0.284	73.722
BLACK 0961C	Polyethylene	0.641	0.644	0.599	28.576
9084C	Polyethylene, chlorinated	0.685	0.690	0.696	19.924
9084C	Polyethylene, chlorinated	0.711	0.716	0.700	23.245
8003C	Polyethylene, chlorinated	0.696	0.700	0.696	21.646
8003C	Polyethylene, chlorinated	0.521	0.512	0.401	46.978
P9-14U	Polyethylene, chlorinated	0.594	0.591	0.520	35.143
P9-14U	Polyethylene, chlorinated	0.518	0.505	0.406	45.822
2474UP	Polyethylene, chlorinated	0.651	0.657	0.514	43.658

2474UP	Polyethylene, chlorinated	0.631	0.635	0.582	29.806
873C	Polyethylene, chlorinated	0.558	0.552	0.452	42.346
873C	Polyethylene, chlorinated	0.557	0.535	0.305	72.557
P9-6C	Polyethylene, chlorinated	0.626	0.603	0.321	76.175
2443UP	Polyethylene, chlorinated	0.503	0.492	0.313	63.161
877C	Polyethylene	0.323	0.274	0.095	113.801
P9-11U	Polyethylene, chlorinated	0.723	0.726	0.689	26.640
BLACK 0961U	Polyethylene, chlorinated	0.734	0.734	0.477	58.856
BLACK 0961U	Polyethylene, chlorinated	0.603	0.609	0.597	22.599
P9-15U	Polyethylene, chlorinated	0.545	0.543	0.498	31.018
P9-7U	Polyethylene, chlorinated	0.595	0.593	0.399	56.852
P9-7U	Polyethylene	0.557	0.542	0.282	76.114
P9-13U	Polyethylene	0.523	0.512	0.296	69.198
P9-13U	Polyethylene, chlorinated	0.584	0.590	0.369	60.147
10112C	Polyethylene, chlorinated	0.622	0.622	0.455	50.208
10112C	Polyethylene, chlorinated	0.653	0.665	0.557	36.668
2469CP	Polyethylene	0.619	0.621	0.543	34.663
2469CP	Polyethylene, chlorinated	0.431	0.405	0.156	95.089
2470U	Polyethylene, chlorinated	0.469	0.411	0.156	105.506
2470U	Polyethylene, chlorinated	0.682	0.685	0.605	33.581
8040C	Polyethylene	0.661	0.659	0.536	41.927

8040C	Polyethylene, chlorinated	0.687	0.697	0.686	21.610
8002C	Polyethylene, chlorinated	0.692	0.696	0.702	20.123
8002C	Polyethylene, chlorinated	0.546	0.537	0.487	33.772
2471UP	Polyethylene, chlorinated	0.665	0.668	0.597	32.455
2471UP	Polyethylene, chlorinated	0.643	0.644	0.567	34.236

## **Actividades desarrolladas durante la realización del TFG**

Observación de las distintas muestras recogidas en campañas realizadas con anterioridad por la doctoranda Bárbara Abaroa y el conteo de los diferentes materiales encontrados en dichas muestras. El principal objetivo es la identificación de microplásticos, además, se contabilizan fibras, óxido, nylon y pintura de barco. Además, se realizó el mismo procedimiento para muestras que recogí durante la realización de dos campañas oceanográficas: PLOCAN 19-1 y VULCANA 0319.

Por otro lado, determinar el PANTONE®, mediante la aplicación móvil PANTONE® Studio, de muestras de microplásticos que fueron obtenidas con anterioridad. Esas muestras, una vez tenga el PANTONE®, se les determina su composición, haciendo uso de FTIR, y su colorimetría, haciendo uso de un colorímetro, para finalmente calcular el Yelowness Index.

## **Formación recibida**

La Dra. Daura Vega impartió un curso donde se ha explicado cómo utilizar las bases de datos para la correcta búsqueda de bibliografía, así como indicar las referencias bibliográficas utilizando para ello el programa Mendeley.

## **Nivel de integración e implicación dentro del departamento y relaciones con el personal**

Tanto en lo que refiere al nivel de integración dentro del departamento como las relaciones con el personal ha sido todo perfecto. Me trataron en todo momento como a una más. Además, existió muy buena relación tanto con la doctoranda que se encontraba en el departamento como con los alumnos de ingeniería química que también realizaban el TFG.

## **Aspectos positivos y negativos relacionados con el TFG**

Como aspectos positivos tengo que destacar todo lo aprendido. La Dra. Daura Vega, se ha preocupado de enseñarme y ayudarme con todo este trabajo. También destacar a la doctoranda Bárbara Abaroa, que gracias a ella he aprendido como muestrear y analizar

resultados. Este trabajo permite saber que es un proyecto de investigación y ayudarte a conocer si es realmente o no lo que quieres hacer en un futuro, entre otras muchas cosas.

Como negativo, lo único que puedo destacar es el tiempo. Es necesario realizar unas prácticas externas para poder desarrollar todo el trabajo, y a veces por motivos ajenos a tutores e incluso a mí, este tiempo es demasiado corto para todo lo que conlleva un TFG.

### **Valoración personal del aprendizaje conseguido a lo largo del TFG**

Como he comentado en aspectos positivos, he aprendido mucho. Sabía que existe un problema con el microplástico, pero no a que nivel.

Aprender a trabajar en equipo, que es muy importante poder contar con buenos compañeros, pero saber que también tienes que ayudar cuando ellos lo necesiten.

Realizar un proyecto del que contamos con “poca” información y llegar a desarrollarlo.